

Determination of the wear resistance of 1020 steel superficially treated in contact with 3104 aluminum alloy using the microwear test compared to the designed wear test evaluated by the moiré optical technique

Fabio Soares¹ , Marcos Dorigão Manfrinato^{1,2} , Jonathan Gazzola³ , Luciana Sgarbi Rossino^{1,2} 

¹Universidade Federal de São Carlos. Campus Sorocaba, Rodovia João Leme dos Santos, Km 110, Bairro do Itinga, 18052-780, Sorocaba, SP, Brasil.

²Faculdade de Tecnologia de Sorocaba. Av. Engenheiro Carlos Reinaldo Mendes, 2015, Alto da Boa Vista, 18013-280, Sorocaba, SP, Brasil.

³Universidade Federal de São Carlos. Campus Araras, Rodovia Anhanguera, Km 174, SP-330, 13600-970, Araras, SP, Brasil.
e-mail: fabio.soares.fs@gmail.com, marcos.manfrinato@fatec.sp.gov.br, jonathan.gazzola@ufscar.br, luciana.rossino@fatec.sp.gov.br

ABSTRACT

The AA 3104 aluminum alloy is widely used as packaging for food storage. However, the package fabrication causes wear to the cutting knife and stamping tools. The objective of this work was to evaluate the wear resistance of the 1020 steel applied in tools for molding and cutting operations of AA 3104, with and without surface treatment, comparing two techniques of wear tests. The samples of 1020 steel were treated by plasma nitriding and DLC film deposition. All samples were tested by a microwear test by fixed ball (MWT). Also, a prototype of the tools machine was developed to simulate the wear between 1020 steel against AA 3104 that occurs in service, whose wear result was analyzed by the moiré optical technique by phase-shifting (DWT). It was observed that the treated samples increased the wear resistance compared to the base material (BM), indicating an increase in the cutting tool lifetime. The DLC film treatment presented greater wear resistance than the nitriding treatment. The microwear test presented the wear volume behavior similar to the behavior of the prototype of wear test, showing that the MWT can be used to study the wear phenomenon with good relationship with the practice, the DWT can indicate the wear behavior of the material in service and the moiré technique can be efficiently used to determine a wear behavior in the designed wear test.

Keywords: DLC film; Plasma nitriding; Wear; Moiré technique.

1. INTRODUCTION

AISI 1020 is a carbon and low-alloy steel, which is a cheap material that presents a good combination of strength and ductility widely used in the manufacturing of simple constructions and machine elements, like piping, construction area, and industrial sheet steel [1–5]. This material is also widely used in the manufacturing of structural components [6] and in stamping tools, knives and cutting punches in eccentric presses for stamping packaging made from AA 3104 aluminum alloy.

AA 3104 is an aluminum-manganese system alloy not-heat treatable thermally, with silicon, magnesium, and iron as the main alloy elements, that presents good corrosion resistance, good conformability, and moderate mechanical strength [7]. This alloy can be stamped and extruded due to its malleability property, promoting premature wear in the cutting knife and stamping tools made of AISI 1020 steel, which arises due to the contact that occurs during the conforming operation of disposable food packaging.

As discussed in the review paper developed by JONSSON *et al.* [8], for a tooling company, knowledge and experience is an important competitive advantage, and to stay competitive in this market there is a need for more efficient processes, systems, tools and supports. For the stamping and cutting operation, the mechanical solicitation is high, and it requires tools produced from steel with strength and tenacity, in which the tribological solicitations of the surface must also be considered [9, 10]. The wear is one of the five main failure mechanisms encountered in the metal tooling [11], and the damage and wear of the tool surface increase maintenance costs and deteriorate the surface quality of the sheet shape products [12].

Wear is an old as time phenomenon, presently being one of the three main industrial problems that lead to the replacement of engineering components and equipment. The wear is rarely catastrophic; however, it reduces the operational efficiency due to the loss of the equipment power, increasing the consumption of lubricant oil and the component substitution to maintain the quality of the product, and thus it is quite undesirable in manufacturing process [13–16]. As presented by NAVARRO-DEVIA *et al.* [15], the tool lifetime improvement and workpiece quality are extremely significant for industrial applications once the cutting tools are an important consumable and indicate the manufacturing growth in a country's economy.

An efficient alternative to improve the surface properties of the steel and increase the lifetime of components that suffer wear in service are the surface treatments [2, 14, 15, 17]. As shown by SELÇUK *et al.* [2], the surface treatments of carburizing, carbonitriding and boronizing improved the hardness and wear resistance of the 1020 steel.

Since the ion beams have been used in full-scale, the surface treatment by plasma has been successfully applied in the tooling industry [18]. As discussed by COSTA *et al.* [10], plasma-assisted surface treatments are efficient in the increase of the hardness, wear, and corrosion resistance of different kind of steels, complying with the necessity of the industrial sector that requires the increase of productivity. The use of plasma nitriding proved to be feasible for M2 and D2 tool steels [10].

Other treatment used to increase the hardness and wear resistance of the metals besides the plasma nitriding is the DLC film deposition by PECVD [15]. The plasma nitriding increased considerably the wear resistance of the P20 steel, mainly used in plastic molds [19], while the DLC film, besides increasing the hardness and wear resistance, decreased considerably the friction coefficient of the Ti6Al4V [20].

Some techniques are used to predict the wear resistance of the materials, as studied by ALTAY *et al.* [21], that used the experimental wear losses under different loads and sliding distances of the AISI 1020 steel surfaces coated with 50FeCrC-20FeW-30FeB and 70FeCrC-30FeB, using the linear regression (LR), support vector machine (SVM), and Gaussian process regression (GPR) algorithms used for predicting wear quantities. A success rate of 0.93 was obtained from the LR algorithm and 0.96 from the SVM and GPR algorithms.

As a traditional method to evaluate the wear resistance of materials with surface treatments, the microwear test by fixed ball is cited [22–28]. The microwear test by fixed ball has been used to evaluate the behavior of thin films and volumetric materials in microscale, since the wear volume or wear depth produced in the test is very small. Thus, this test is adequate to determine the wear resistance of thin films and other coats or layers produced by the surface engineering, and, by enabling a wide adjusted range of load, the fixed ball test system is widely used to study the microwear in a variety of materials [29, 30]. In this case, the wear resistance is obtained by the crater analysis formed in the test, being possible to determine the wear mechanism, wear volume, wear rate, and the depth of the crater penetration, to verify if the test reaches the substrate during the test or remains on the treated surface [24, 30–34].

Prototypes that simulate the real wear situation of parts in service can be produced, and wear resistance may be defined by mass loss, as well as wear volume may be determined by the scar geometry produced on the test, or by the changing of the part geometry after the test. In the second case, the moiré technique can be an alternative to determine the wear resistance of tested parts using specially designed equipment to simulate a specific wear condition.

The Moiré technique (MT) has been used in a variety of areas, as for example, to evaluate the soil surface [35], to decode information hiding scheme for visual cryptography [36], to digitalize the human body [37], to the measurement of nonlinear optical properties of noble metal nanoparticles [38] and to analyze biological surface profiles and shapes without contact [39].

The MT is a robust, non-destructive, experimental simplicity and contactless methodologies that use low-cost equipment, performed with an accessible method to generate digital images from interference phenomenon created by light gratings projected onto the surface of interest [35].

In this work, a comparison of wear resistance of the AISI 1020 steel with two kinds of surface treatment – plasma nitriding and DLC film deposition – was studied through the microwear test by fixed ball and using a prototype of wear test developed to simulate the contact between the stamping tools made from 1020 against the AA 3104 aluminum alloy. It was possible to observe whether the surface treatments can improve the wear resistance of the material. The two kinds of wear tests were evaluated, being possible to determine whether the laboratory test can efficiently set the wear behavior that occurs in the test using a prototype wear equipment analyzed by moiré optical technique.

2. MATERIALS AND METHODS

Two kinds of AISI 1020 steel samples were produced, as presented in Figure 1. The round sample (Figure 1(a)) was used to carry out the microwear test by fixed ball, and the triangular sample (Figure 1(b)) was used in the wear test carried out by the prototype developed.

The geometry and dimension of the triangular sample were defined to be as similar as possible to the stamping and cutting tools used in the packaging fabrication process. All the samples were abraded with the use of water sandpaper, polished with 3 μm diamond paste, cleaned in an ultrasound equipment with detergent and isopropyl alcohol for 5 min each stage, and dried with the use of a thermal blower.

2.1. Surface treatments

The surface treatments were carried out in plasma equipment using a pulsed-DC power supply in the Laboratory of Technology and Surface Engineering (LabTES) of Sorocaba Technological College (Fatec-Sorocaba) located in Sorocaba, São Paulo – Brazil. A detailed description of the equipment is presented in CRUZ *et al.* [40].

The cleaning of the samples by plasma ablation process was carried out before all surface treatments, using Ar (80%) and H_2 (20%) gases at a pressure of 2.0 torr for 60 min, in the temperature of the treatment.

The nitriding treatments were carried out with a fixed parameters of 550°C, 5 hours, in a pressure of 7 torr and gas flow at 500 sccm, varying the gas proportion for each of the two studied treatments: 80% N_2 – 20% H_2 (80N) and 60% N_2 – 40% H_2 (60N).

To the DLC film deposition, carried out by PECVD technique using a CH_4 as a precursor and Ar as gas excitation; an interlayer was deposited immediately after the cleaning of plasma ablation process using hexamethyldisiloxane (HMDSO) as a precursor in a proportion of 70% HMDSO and 30% Ar for 15 min, voltage of 300 V, temperature of 200 °C and 6.0×10^{-2} torr of total pressure gases. After that, without opening the reactor, the DLC film was deposited with 90% CH_4 and 10% Ar at 30 sccm, 500 V, 4.16×10^{-1} torr for 2 hours.

2.2. Samples characterizations

The samples with nitriding treatment were characterized by metallography, X-ray diffractometry (XRD), and hardness profile. The sample with DLC film deposition was characterized by Fourier transform infrared spectroscopy (FTIR) and Raman spectroscopy analysis.

For metallographic analyses, the nitrided samples were cut in a transversal direction, embedded in high adhesion Bakelite, sanded, polished, and attacked with Nital 3%. The micrography analyses were obtained by Leica model DMI8 C optical microscopy with camera and software of capture and image analysis.

The X-ray diffraction (XRD) analyses were performed on the nitrided samples using Siemens equipment, model D5005. The source voltage and an amperage of 40 kV and 30 mA were used, respectively, using a $\text{CuK}\alpha$ ($\lambda = 1,54056 \text{ \AA}$) radiation with a 0.02° step and 2θ ranging from 5° to 90° . The diffractograms were analyzed using the Crystallographica Search – Match software, to find the phases formed for each peak of the obtained diffractogram.

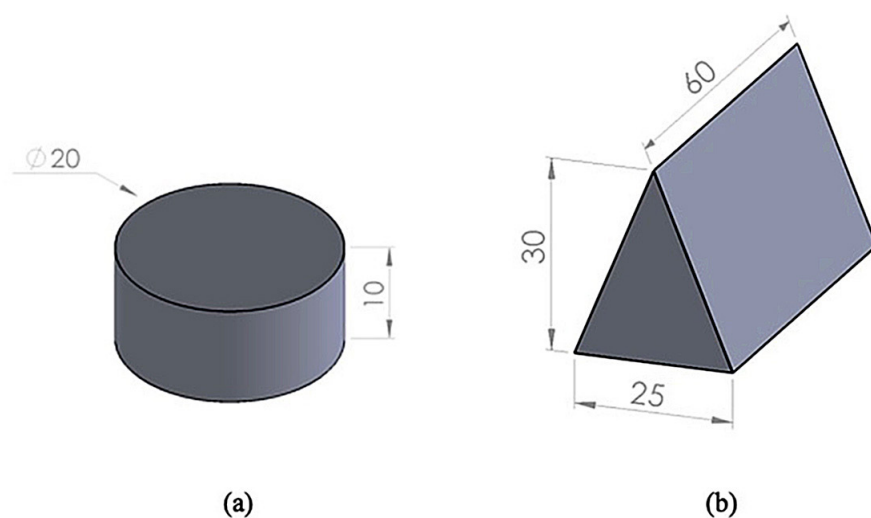


Figure 1: Geometry and dimension (mm) of the samples used to (a) microwear test by fixed ball and (b) wear test using a prototype of wear equipment.

The hardness profile was carried out to obtain the hardness in the depth of the layer formed in the plasma nitriding treatment, determined by Vickers (HV) microhardness tests using a Mitutoyo model HM 220 with a load of 0.01 kgf.

The determination of the compounds and bands formed in the DLC film was defined by Fourier transform infrared spectroscopy (FTIR) carried out using JASKO FTIR-410 Spectrometry equipment. The scanning time was 128 s on the range of 4000 at 400 cm^{-1} and a resolution of 4 cm^{-1} .

The surface roughness of the treatments was determined by profilometry using a VeecoDektak 150 equipment exerting a force of 3.00 mg and time of 12s on the surface with horizontal scanning of 650 μm and resolution of 0.056 μm .

The D and G bands of the DLC film were analyzed by Raman Spectroscopy using an argon laser with 5 μm of diameter spot, the wavelength of 514 nm, and power of 5% in a Renishaw-in Via Raman Microscope. The obtained spectra were deconvolved by the Fityk 0.9.8 software and the extracted data was analyzed using Origin Software 6.0. The ratio between the intensity bands D and G (ID /IG), the G band displacement, and the width of half of band G (FWHM(G)) were determined to obtain the microstructure information of the film [41]. To derive the hydrogen content in film, it was used equation (1) [42].

$$H(\%) = 21.7 + 16.6 \log \frac{m}{I(G)[\mu\text{m}]} \quad (1)$$

where I(G) is the intensity of G band and m is the inclination of spectra between 1000 and 1800 cm^{-1} .

2.3. Microwear test by fixed ball (MWT)

The microwear test was carried out in the samples with and without treatment using a fixed ball device shown in Figure 2, more detailed in RANGEL *et al.* [43].

The wear test was carried out using a sphere or fixed ball of AISI 52100 steel with radius R of 12.7 mm with a rotation frequency fixed at 1194 rpm, with a normal load of 8 N and time of 600 s. After the test, the diameter of the wear crater (d) was measured by Leica model DMi8 C optical microscopy (MO) to estimate the wear volume (V), determined in equation (2) [44]. The tests were carried out in triplicate, without any lubricant or abrasive slurry, to keep the similarity to the DWT test.

$$V = \frac{\pi * d^4}{64 * R} \quad (2)$$

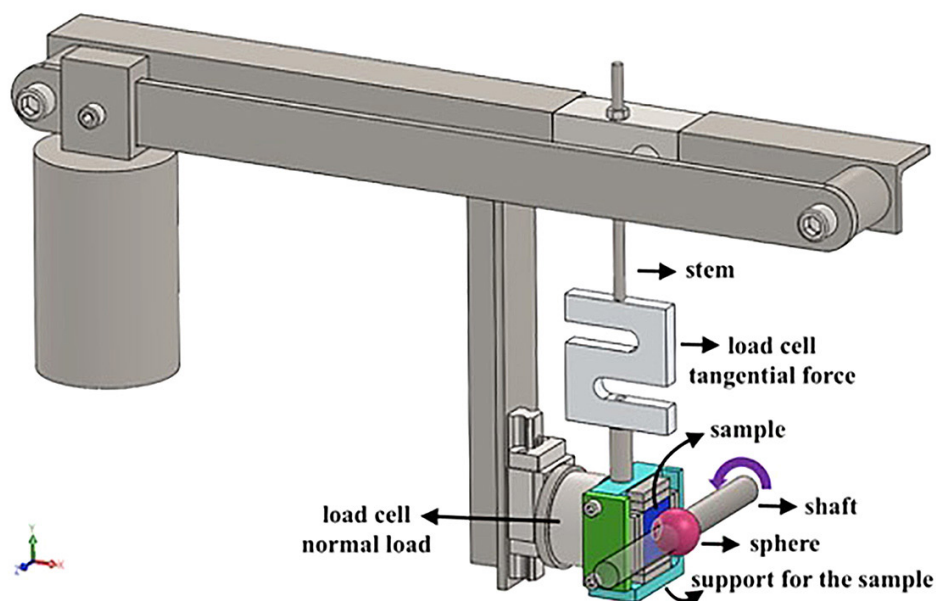


Figure 2: Illustrative scheme of the microwear equipment by fixed ball.

2.4. Wear test by prototype developed and moiré technique (designed wear test – DWT)

A device, shown in Figure 3, was developed to reproduce the wear that occurs in the cutting and stamping process suffered by the AA 3104 aluminum alloy due to its contact with the press and knife made of 1020 steel. The contact between the plate of AA 3104 aluminum alloy (counter-body) with the body (1020 steel) is accomplished by the two pressure springs. The sliding between the body and counter-body is performed in linear oscillatory movement through a pneumatic cylinder. Each test on the body with and without surface treatment was carried out at 11.000 sliding cycles, and the load of 27 kgf was applied by the compression of the springs situated on the top of the device, leaving the length of both at 55 mm to reproduce the real situation. The analysis of the wear produced sample after the test was carried out by the moiré optical technique by phase-shifting, as recommended by DAL FABBRO *et al.* [45]. This technique allows digitizing the complete topographic profile of objects, thus determining their volumetric loss.

The phase-shifting moiré optical technique is based on the projection of 4 white and dark grids outdated of $\frac{1}{4}$ of the period between each other projected on the background and the specimen. Image digital processing allows getting the topographic profile of the studied object, as shown in Figure 4. Therefore, the difference of the

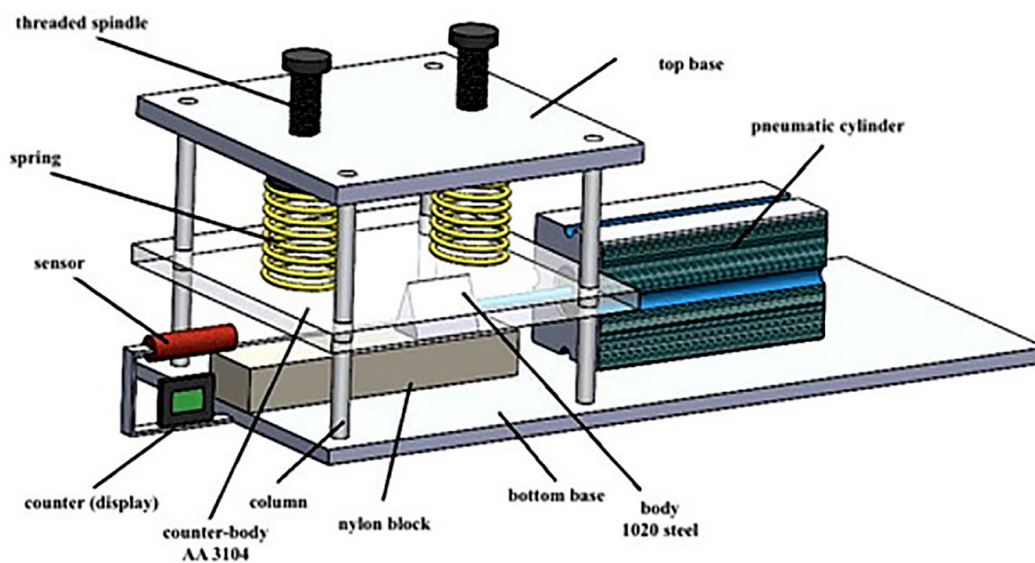


Figure 3: Illustrative scheme of the prototype of the wear equipment developed to simulate the real situation that occurs in the molding process occurred between the 1020 steel against the AA 3104 aluminum alloy.

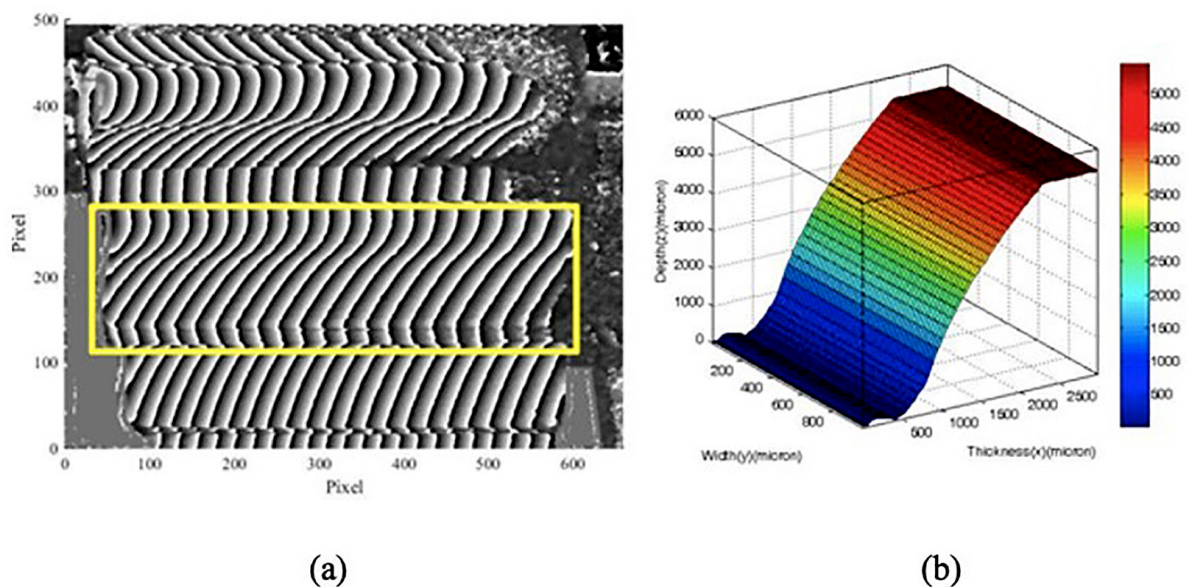


Figure 4: Moiré shape survey image processing and 3-D gear tooth reconstruction obtained by Moiré technique [46].

topographic profiles of the wear and not wear samples allows to determine the reduction of the height suffered by the wear sample and, consequently, provides the data to calculate the wear volume of the piece.

In this work, the grids were generated by Fringe Projection[®] software and projected through multimedia projector connected to a computer. Samples were painted with thin layer of matte white spray paint to increase the contrast with the projected grid. Initially, the 4 outdated grids were projected on a white background. Subsequently, one of the grids was projected on the wear sample with and without treatment. Then, for each sample, a set of 5 images were captured through a Samsung cell phone model Galaxy J5 with 13 megapixels of resolution and triggered via Bluetooth to avoid any movement of the camera. The analysis of the images was carried out by ImageJ[®] software version 1.64R and by the software Rising Sun[®] version 1999/2000, in accordance with SANTOS *et al.* [47]. It is important to note that the use of the paint is necessary to achieve better grid contrast in the use of the moiré technique, and all the samples were submitted to the wear test in the same conditions [47–50].

The frontal and lateral wear profile of the sample is represented in Figure 5, in that the dashed line represents the wear region to be evaluated (analysis line).

The profile conversion generated by the moiré technique from pixel to millimeters serves as a basis for determining the material wear volume, following the procedures recommended by SANTOS *et al.* [47]. The pixel height data of the wear sample along its length was obtained through the ImageJ[®] software. The millimetric height of the wear sample was determined with a caliper, choosing its end as the reference point. Equation (3) determined the conversion ratio ($R_{x,y}$) relating known point in millimeter ($H_{x,y}$) with its pixel height of the wear sample ($P_{x,y}$). Subsequently, this ratio was applied to convert height pixel data in millimeters (y) along its length (x).

$$R_{x,y} = \frac{H_{x,y} [mm]}{P_{x,y} [pixel]} \quad (3)$$

To determine the wear volume of the samples, it was adopted that the profile between the areas was linear and the isosceles triangular shape, as observed on wear specimens, and illustrated in Figure 5(b) and Figure 6. Thus, the precision of the wear volume calculated by the adopted technique is related to the accuracy of the point capture ($A_{x,y}$), which is the relationship between the total length of the sample ($C_{x,y}$), in millimeters, by the length of the object digitally reconstructed ($L_{x,y}$), in pixels.

Wear volume (V_{total}) was calculated in function of wear area determination ($A_{wear\ area}$). Equation 04 determined tangential angle of triangle inclination ($\tan \theta$) based on the without wear shape sample. Equations 05, 06 and 07 determined area profile with wear height ($H_{wear\ height}$) determined by differences of millimetric height between samples with wear and without wear and width of the wear shape specimen (B). Wear volume was calculated summing parcels of each wear volume profile ($V_{wear\ volume}$) through equations 08 and 09.

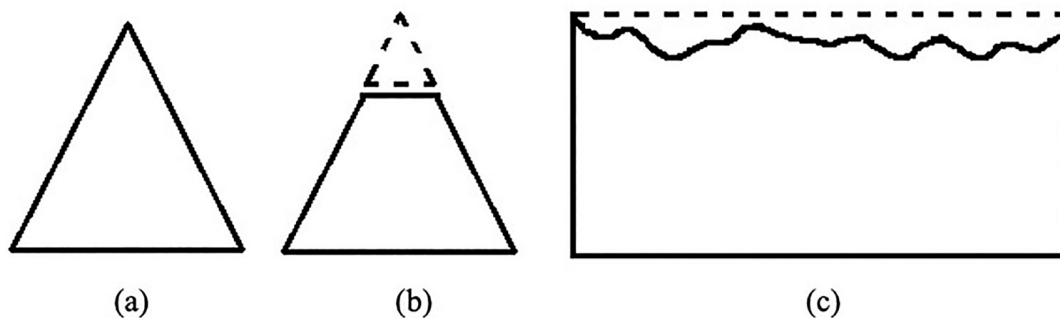


Figure 5: Sample profiles (a) without wear, (b) frontal wear and (c) lateral wear.

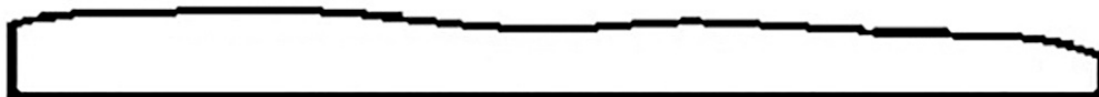


Figure 6: Longitudinal wear profile obtained through moiré optical technique shape survey.

$$\tan \theta = \frac{co}{ca} = \frac{H_{total}}{b/2} \tag{4}$$

$$H_{wear\ height} = H_{total\ height} - H_{moiré\ height} \text{ (mm)} \tag{5}$$

$$B_{(wear\ base)} = 2 * \frac{H_{wear\ height}}{\tan \theta} \text{ (mm)} \tag{6}$$

$$A_{(wear\ area)} = \frac{B_{(wear\ base)} * H_{(wear\ height)}}{2} \text{ (mm}^2\text{)} \tag{7}$$

$$V_{(wear\ volume)} = A_{(wear\ area)} * L_{(profile\ width)} = A_{x,y} * A_{(wear\ area)} \text{ (mm}^3\text{)} \tag{8}$$

$$V_{total} = V_1 + V_2 + V_3 + V_4 + \dots + V_n \text{ (mm}^3\text{)} \tag{9}$$

3. RESULTS AND DISCUSSIONS

3.1. Characterization of the treated materials

The characterizations of the produced DLC film were done by FTIR and Raman spectra analysis. The FTIR spectrum obtained for the formed DLC films, observed in Figure 7(a), shows the formation of bond and functional groups characteristic of DLC film. It is possible to observe the presence of band C ≡ C at the

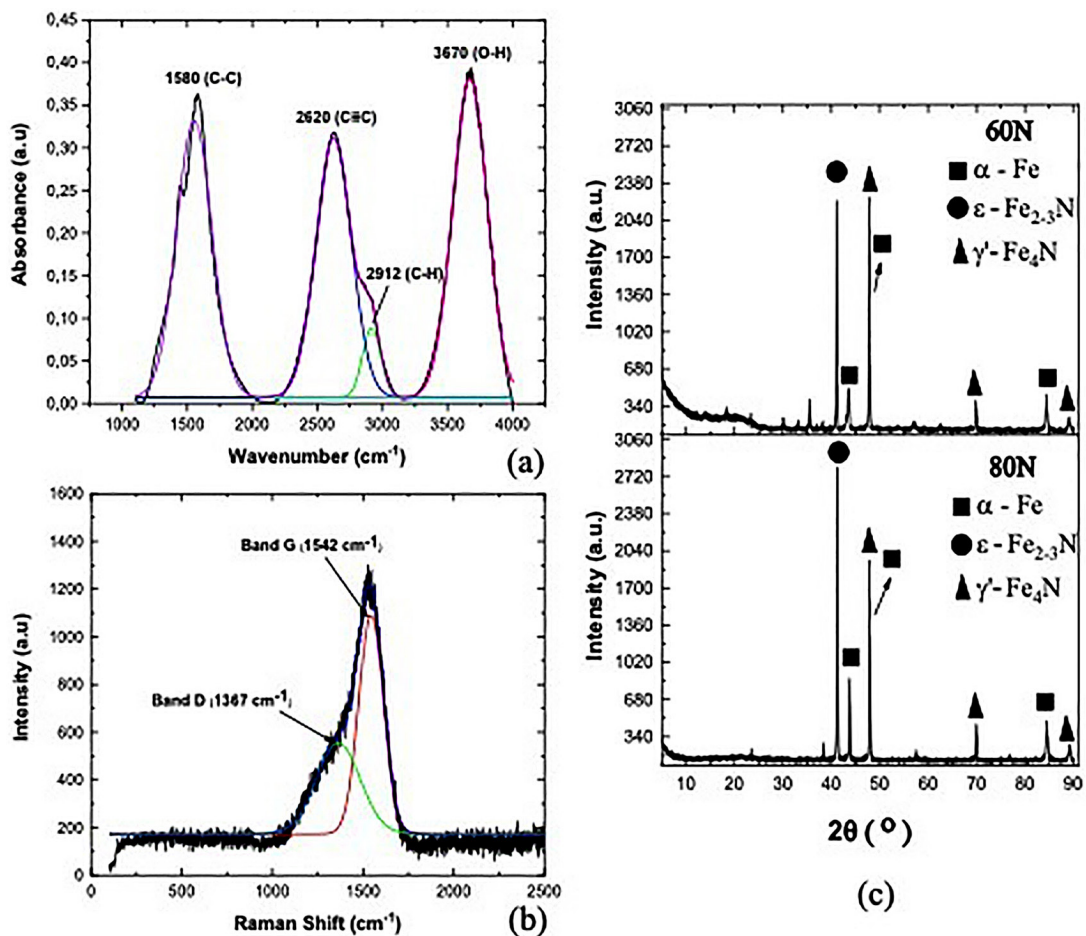


Figure 7: Analyze of (a) FTIR spectrum for the DLC film (b) Raman spectrum for the DLC film (c) Diffractograms for the nitrated materials.

wavenumber of 2620 cm^{-1} and the band C–C at the wavenumber of 1580 cm^{-1} . The band with low intensity observed at the wavenumber of 2912 cm^{-1} is related to the C–H² bond that obtains a higher concentration of sp³ [41]. The wave number of 3670 cm^{-1} is related to the O–H bond from the ambient humidity.

The DLC film was deposited with a high percentage of CH₄ due to the fact that, as observed by ALMEIDA *et al.* [20], the lowest percentage of methane produces a thinner film than a higher percentage of methane, explained by the high ionization potential of this gas, which decreases the deposition rate of the film [41]. Then, this gas must be higher in percentage than argon to form a good thicker film.

Figure 7(b) shows the Raman spectrum of the DLC film produced in this work, which indicates the formation of a hydrogenated amorphous carbon film [20]. The G band, found in 1560 cm^{-1} , is related to sp² bond, characteristic of graphitic materials, and the D band is found in 1380 cm^{-1} , related to angular alteration of sp² bond, that occurs due to the presence of sp³ hybridization. It was possible to observe a displacement of the D and G band for smaller Raman shift, with values of 1367 and 1542 cm^{-1} respectively, meaning that there was amortization of the film related to the sp² bond, corresponding to the increase of the bond related to sp³ hybridization [41].

As presented by ROBERTSON [41] and discussed by CASIRAGHI *et al.* [42], the relation between the A(D)/A(G) ratio with FWHM to G band can determine the kind of film produced. Low values of FWHM with a low A(D)/A(G) ratio determine a polymeric-kind film formation (PLCH). To high A(D)/A(G) ratio with low values of FWHM, the kind of film formation is graphitic (GLCH or GLCHH). The kind of film formed in this work is DLCH, in that A(D)/A(G) ratio is 0.76 with an intermediated value of FWHM (161.3 a.u. to G band), containing the presence of microcrystalline graphite rings and chains with a transition between amorphous carbon with a higher concentration of C–C sp² bond [42].

In accordance with ROBERTSON [41], the a-C films are characterized by the I(D)/I(G) ratio lower than 1. Analyzing the I(D)/I(G) ratio of 0.42 and the hydrogen percentage of 33.4%, it is possible to characterize the DLC films produced in this work as a-C:H hard, considering the classification proposed by ROBERTSON [41].

The compound layer formed in the nitriding treatment is shown in Figure 8, with a thickness of $25.5\text{ }\mu\text{m}$ to the 80N treatment and $22.98\text{ }\mu\text{m}$ to the 60N treatment. It is possible to observe two kinds of phases forming the compound layer.

As discussed by YANG [51] and observed by DANELON *et al.* [52], the substrate region close to the surface is rich in nitrogen, favoring the $\epsilon\text{-Fe}_{2-3}\text{N}$ phase formation. Due to the differences in the flux of nitrogen leaving from the interfaces, the phase $\gamma'\text{-Fe}_4\text{N}$ is formed below the $\epsilon\text{-Fe}_{2-3}\text{N}$ phase, once the formation of the $\gamma'\text{-Fe}_4\text{N}$ phase is favored for a lower percentage of nitrogen [51].

These phase formations are proven by XRD analysis, shown in Figure 7(c). The peaks of the $\epsilon\text{-Fe}_{2-3}\text{N}$ phases are more intense in the 80N treatment compared to the 60N treatment. The phase $\epsilon\text{-Fe}_{2-3}\text{N}$ is formed by increasing of nitrogen concentration in the treatment. Then, the condition 80N presented the thickest $\epsilon\text{-Fe}_{2-3}\text{N}$ phase. This result corroborates with the metallography analysis.

The hardness profile is also influenced by the nitrogen flux applied in the treatment, as observed in Figure 9. It is possible to observe the increase in the surface hardness without interfering in the substrate, keeping it ductile. The 80N produced a thicker layer with the thicker $\epsilon\text{-Fe}_{2-3}\text{N}$ phase formation, which influenced the

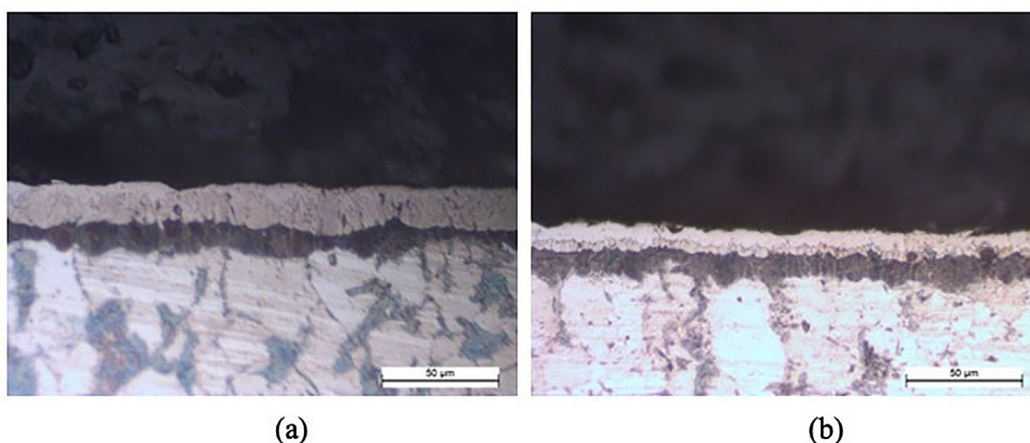


Figure 8: Micrography of the compound layer formed in the nitriding treatment (a) 80N, (b) 60N.

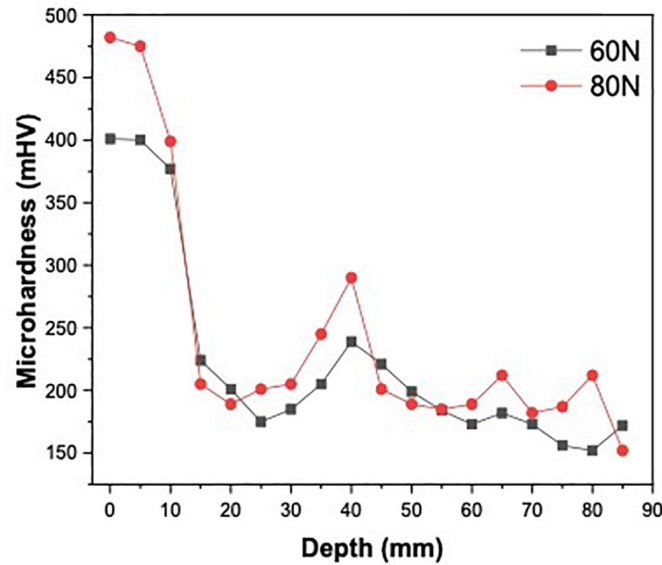


Figure 9: Hardness profile of nitrided materials.

higher hardness obtained in this treatment. In the literature it is possible to find works [53–55] that corroborate with the hardness effect of the ϵ -Fe₂₋₃N. Also, the high hardness on the surface is related to compound layer formations and the profile of hardness decreases explained by the decrease in the nitrogen concentration in depth [33, 40].

3.2. Results of the wear test

The behavior of the material with and without treatments at the MWT is observed in Figure 10(a), showing that all treated materials present better wear resistance than the base material (BM), once the high hardness is one of the important properties to the tool steel for achieving good resistance to abrasive wear [11]. Although all treatments are effective in the wear resistance of the material, a lower wear volume was observed by the material with DLC film deposited. As discussed in CAMPOS *et al.* [27], the highest wear resistance shown by DLC film is due to the high hardness and low friction coefficient of this kind of film, being considered as a solid lubricant. This property of the DLC film is indicated by the roughness value of $72,7 \text{ nm} \pm 4,12$, lower than the nitrided samples, that presented roughness values of $124,4 \text{ nm} \pm 5,67$ and $141,1 \text{ nm} \pm 3,07$ for the 60N and 80N samples, respectively.

As discussed in FOLLE and SCHAEFFER [56], the lubricant has an important role in the stamping process, due to the reduction of the friction coefficient that reduces the premature fracture and localized thinning of the sheet thickness. Also, some solid lubricant can be applied in metals to reduce the friction coefficient, as teflon [57], nylon and rubber [58].

The influence of a few operative variables in the friction coefficient was investigated by FRATINI *et al.* [57], as the specimen material (AA1050, Fe-P01, AISI 304, brass and copper), the pin diameters that has influence on the contact pressure (25 and 50 mm), the tooling pin surface finish (machined and chromed) and the lubricating conditions (dry, EP grease and Teflon). The effect of the tooling pin surface finish and contact pressure showed depending on the utilized specimen material, but for all of them, the use of Teflon lubricant condition, independent of machined or chromed surface finish, presented the lowest friction coefficient. This is justified by the fact that Teflon acts as a solid lubricant, and when a liquid lubricant cannot be used, a surface modification is indicating to develop the wear protection of the metals [59].

Thus, the DLC develops this effect, without contaminating the AA 3104 aluminum alloy used as the packaging for food storage studied in the specific situation of this work, as it would be possible when using a liquid lubricant.

ARAÚJO *et al.* [16] observed that the plasma nitride treatment carried out at forming tool made by traditional AISI-M2 high-speed steel used to the nails production shows a significant increase in the nails production preventing the premature wear and tearing of the material, increasing the tool lifetime. The wear resistance determined by the sliding wear test presented the similar behavior observed in the manufacturing

process. It suggests that wear test can denote the wear behavior of the material applied in service. The result observed by ARAÚJO *et al.* [16] corroborates with the results obtained in this work.

Although the 80N treatment presented a thicker and harder layer, the 60N treatment showed better wear resistance. KAMARIS [60] observed that the wear resistance decreases with the increase in the compound layer thickness since the thicker compound layer has a porous and fragile structure. Also, the ϵ -Fe₂₋₃N phase, existing in greater intensity in the 80N, is brittle in nature, which cannot support the loads without cracking, and it can increase the wear volume of the material [16].

Considering that the life of tool steel is generally governed by design, material, heat treatment, manufacturing techniques, work material, production conditions and maintenance of press tool components [8, 11], it is possible to accomplish in this study that one alternative to increase the tool life can be obtained from surface treatments, mainly in AISI 1020 steel used to forming and cutting the AA3104 aluminum alloy.

The wear behavior obtained by simulating the practice is important to ensure reliable results. This situation was obtained in the DWT using the MT. The analysis of the results of the wear volume using the MT presented in Figure 10(b) allows us to observe that both the nitriding treatments and the deposition of the DLC film promote a better resistance compared to 1020 steel without treatment when in contact with the aluminum alloy AA 3104. Also, in this case, the DLC film presented better wear resistance than the nitriding treatment, and the 60N presented lower wear volume than the 80N treatment. Even though the wear volume obtained in the DWT may have overtaken the surface treatment, reaching the substrate during the test, probably the treatments were successful in providing the lower wear rate in the initial portion of the test, keeping the total wear volume lower than the base material. This behavior evidences the effectiveness of the surface treatments even under severe wear solicitations.

The quantify analyses of the lateral profile of the studied samples obtained after the DWT test is presented in Figure 10(c), whose characteristics generated by the image software are shown in Figure 11. It is possible to observe that the BM showed the smallest height compared to treated materials, confirming the greater resistance provided by the surface treatments of nitriding and DLC film deposited on the AISI 1020 in contact with the AA 3104 aluminum alloy.

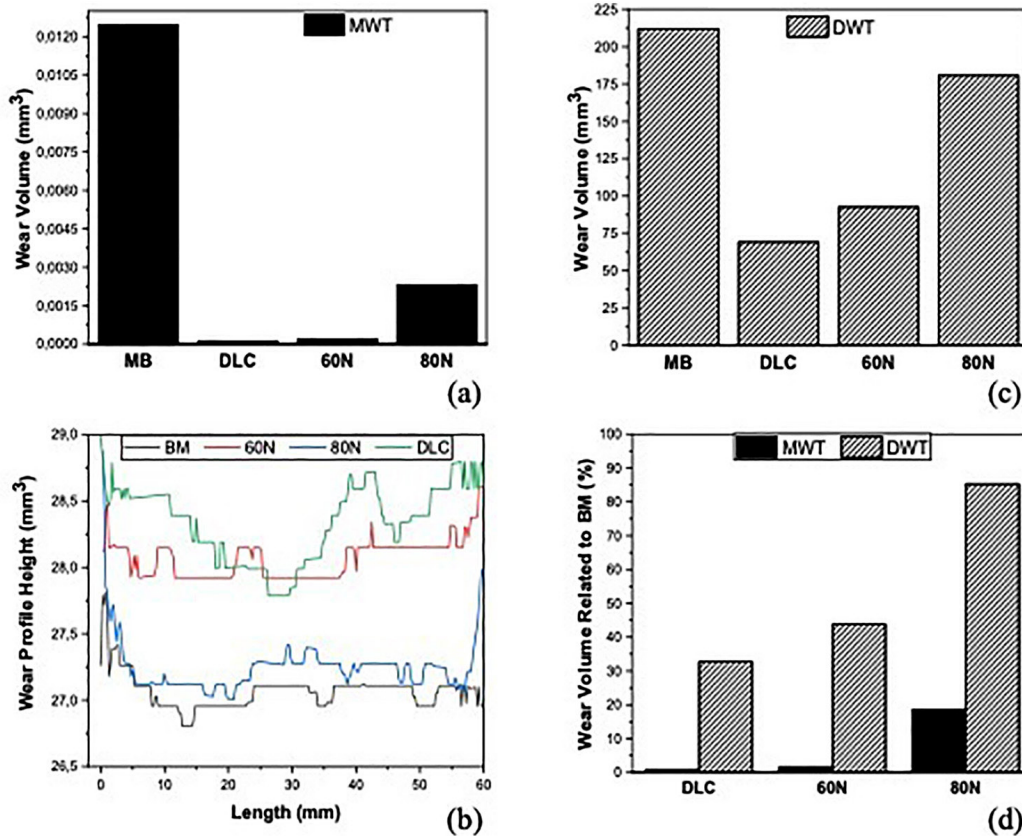


Figure 10: Wear behavior of the material with and without surface treatment in the (a) MWT (b) DWT (c) wear profile height obtained in the DWT and (d) comparison of the results in the wear tests.

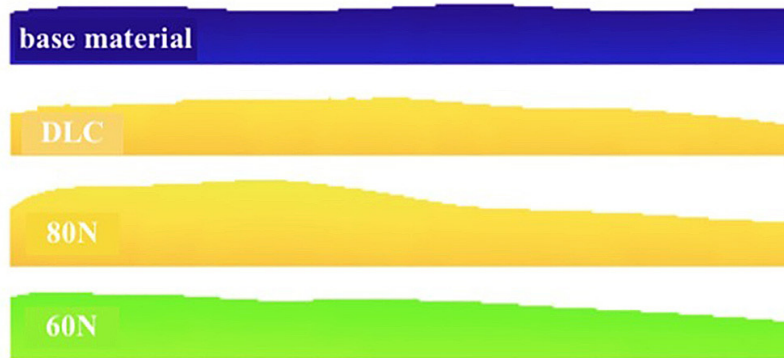


Figure 11: Characteristics of the lateral profile of the samples with and without treatments after DWT.

Figure 10(d) shows the degree of wear volume in relation to the total volume of the sample for each treatment analyzed. This analysis index is a percentage between the wear volume, obtained in the experimental test, in relation to the volume of the base material. Comparing this index, it is noticed that the wear trend between the treatments is in common agreement, i.e., the MWT with the test carried out with the DWT analyzed with the MT, the DLC bodies are more resistant, followed by the 60N treatment and the 80N treatment, respectively.

Despite the different values and the highest wear percentage obtained to the DWT due to the higher severity of the test, it is possible to observe that for both wear tests the volume follows the same sequence of growth, which contributes to the validation and reliability of wear tests and the results presented by them. This shows that surface treatments, when subjected to similar parameters in different kinds of tests, tend to show proportional wear results between them. Figure 10 (d) shows for both kinds of test (MWT and DWT) an increase in the wear volume of the treated samples, complying with the sequence of $DLC < 60N < 80N$.

The wear process is complex and depends on a number of factors [61]. However, it is possible to perform an extensive study of the effect of the wear parameters in the wear resistance of the material with different surface treatments. On the other hand, the wear test carried out by prototype devices simulates as close as possible the real situation.

We can observe that, although the wear volume obtained in the DWT test was higher than the MWT test, the wear behavior of the 1020 steel, with and without treatment, was similar in both tests. The wear volume obtained in the DWT test is justifying due to the severe wear solicitation occurred in this test, but the surface treatment reproduces the wear behavior in both solicitations.

The effect of the severe wear solicitation in the wear volume obtained in this work is in accordance with PEREIRA NETO *et al.* [33] and SEN [62], that observed that the increase in the contact load increased the wear rate and wear volume for the metals submitted to different surface treatments, explained by the high solicitations occurred in this situation.

These results do not determine the lifetime of the AISI 1020 tool but show the significantly increase in the wear resistance of the treated material compared to untreated material, evidencing the effectiveness of the treatments that indicates its uses in this situation. Also, the results show that the MWT can indicate the efficiency in the study of the wear mechanism, phenomenon and tendency of wear resistance of materials applied in practice while the DWT can be used to evaluate the wear resistance of materials using tests developed to reproduce real situations, studying the behavior of materials that suffer wear in service.

4. CONCLUSIONS

In this work, studies were performed to determine the wear resistance of the 1020 steel with and without surface treatment of DLC film deposition and plasma nitriding treatment. The wear volume obtained in the microwear test by fixed ball presented similar behavior with the results obtained in the prototype developed to simulate the real situation using the moiré technique of 1020 when in contact with 3104 aluminum alloy.

The DLC film produced in this work is related to a-C:H hard due to the percentage of hydrogen of 33.4%, a low value of $I(D)/I(G)$, and the relation between $A(D)/A(G)$ and $FWHM(G)$.

In the nitriding treatment, it was observed that high nitrogen concentrations are able to produce a thicker compound layer and greater thickness of the ϵ -Fe₂₋₃N phase, which is harder than the γ -Fe₄N phase, produced by low concentrations of the nitrogen.

All treatments were effective in improving the wear resistance of the studied material when compared to the base material. This is evidenced both for the microwear test by fixed ball and the prototype developed to simulate the real situation using the phase-shifting moiré technique.

Between the two kinds of treatment studied, the samples with DLC film showed better wear resistance, guaranteeing wear volume 88% lower when compared to nitriding treatment and 95% less compared to the base material, when in contact with AA 3104 aluminum. Also, the higher percentage of nitrogen introduced in the treatment can damage the wear resistance of the material compared to treatment performed with a low percentage of nitrogen, due to the characteristics of the obtained layer feature.

Although the nitriding did not obtain superior results to the DLC films in this work, it can also be used for the superficial improvement of the 1020 steel knives, since this treatment presented a lower wear volume compared to the samples without treatment.

It is concluded that the results show that the application of the two wear techniques used in this work is effective to determine the behavior of punches or knives made with 1020 steel for cutting AA 3104 aluminum alloy, commonly found in food packaging industries and beverages, for example, being able to extend the lifetime of this equipment. The moiré technique ally to adequate wear equipment developed to simulate a real and specific situation is efficient to measure the wear characteristics and wear resistance of the materials in contact.

5. ACKNOWLEDGMENTS

We would like to thank Capes (finance code 001).

6. BIBLIOGRAPHY

- [1] DIETER, G.E. *Materials selection and design*, v. 20, ASM Handbook, Ohio, CRC Press, 1997. doi: <http://dx.doi.org/10.31399/asm.hb.v20.9781627081948>.
- [2] SELÇUK, R., IPEK, R., KARAMIS, M.B., “A study on friction and wear behaviour of carburized, carbonitrided and borided AISI 1020 and 5115 steels”, *Journal of Materials Processing Technology*, v. 141, n. 2, pp. 189–196, 2003. doi: [http://dx.doi.org/10.1016/S0924-0136\(02\)01038-5](http://dx.doi.org/10.1016/S0924-0136(02)01038-5).
- [3] SASH, A., EL-FAWKHRY, M.K., EL RAHMAN, S.A.A., *et al.*, “Improvement of mechanical properties and structure modifications of low carbon steel by inoculations with nano-size silicon nitride”, *Journal of Nano Research*, v. 47, pp. 24–32, 2017. doi: <http://dx.doi.org/10.4028/www.scientific.net/JNanoR.47.24>.
- [4] DEWANGAN, S., MAINWAL, N., KHANDELWAL, M., *et al.*, “Performance analysis of heat treated AISI 1020 steel samples on the basis of various destructive mechanical testing and microstructural behaviour”, *Australian Journal of Mechanical Engineering*, v. 20, n. 1, pp. 74–87, 2019. doi: <https://doi.org/10.1080/14484846.2019.1664212>.
- [5] KUI, C.F., FEI, L.Y., XUE, X.J., *et al.*, “The dynamic characteristics and constitutive model of 1020 steel”, *Emerging Materials Research*, v. 6, n. 1, pp. 124–131, 2017. doi: <http://dx.doi.org/10.1680/jemmr.16.00019>.
- [6] KARAMIŞ, M.B., İPEK, R., “An evaluation of the using possibilities of the carbonitrided simple steels instead of carburized low alloy steels (wear properties)”, *Applied Surface Science*, v. 119, n. 1–2, pp. 25–33, 1997. doi: [http://dx.doi.org/10.1016/S0169-4332\(97\)00173-6](http://dx.doi.org/10.1016/S0169-4332(97)00173-6).
- [7] Associação Brasileira Do ALUMÍNIO, *Fundamentos e aplicações do alumínio*, São Paulo, ABAL, 2007, 68 p.
- [8] JONSSON, C.-J., STOLT, R., ELGH, F., “Stamping tools for sheet metal forming: current state and future research directions”, In: *Proceedings of the 27th International Conference on Transdisciplinary Engineering*, pp. 281–290, Poland, July 2020.
- [9] PINEDO, C.E., “Revestimento PVD e nitretação sob plasma aplicados em ferramentas para conformação e corte a frio”, In: *Anais do 9º Encontro da Cadeia de Ferramentas, Moldes e Matrizes*, pp. 99–108, São Paulo, Ago. 2011.
- [10] COSTA, E.S., SOUSA, R.R.M., MONÇÃO, R.M., *et al.*, “Plasma nitriding and deposition in AISI M2 and D2 steel tools used in nail forming and stamping: a viability study”, *Revista Matéria*, v. 26, n. 1, pp. e12922, 2021. doi: <https://doi.org/10.1590/S1517-707620210001.1222>.
- [11] NARANJE, V.G., KARTHIKEYAN, R., NAIR, V., “Study of wear performance of deep drawing tooling”, *IOP Conference Series. Materials Science and Engineering*, v. 244, pp. 012004, 2017. doi: <http://dx.doi.org/10.1088/1757-899X/244/1/012004>.

- [12] BANG, J., PARK, N., SONG, J., *et al.*, “Tool wear prediction in the forming of automotive DP980 steel sheet using statistical sensitivity analysis and accelerated U-Bending based wear test”, *Metals*, v. 11, n. 2, pp. 306, 2021. doi: <http://dx.doi.org/10.3390/met11020306>.
- [13] GAHR, K.H., *Microstructure and Wear of Materials*, v. 10, New York, Elsevier, 1987.
- [14] DAVIS, J.R., *Surface Engineering for Corrosion and Wear Resistance*, Ohio, ASM International, 2001. doi: <http://dx.doi.org/10.31399/asm.tb.secwr.9781627083157>.
- [15] NAVARRO-DEVIA, J.H., AMAYA, C., CAICEDO, J.C., *et al.*, “Hafnium and vanadium nitride multilayer coatings [HfN/VN]_n deposited onto HSS cutting tools for dry turning of a low carbon steel: a tribological compatibility case study”, *International Journal of Advanced Manufacturing Technology*, v. 101, n. 5–8, pp. 2065–2081, 2018. doi: <http://dx.doi.org/10.1007/s00170-018-3020-8>.
- [16] ARAÚJO, A.G.F., NAEEM, M., ARAÚJO, L.N.M., *et al.*, “Design, manufacturing and plasma nitriding of AISI-M2 steel forming tool and its performance analysis”, *Journal of Materials Research and Technology*, v. 9, n. 6, pp. 14517–14527, 2020. doi: <http://dx.doi.org/10.1016/j.jmrt.2020.10.048>.
- [17] HOLMBERG, K., MATTHEWS, A., “Tribological properties of metallic and ceramic coatings”, In: Bharat, B. (ed), *Modern Tribology Handbook*, v. 2, *Materials, Coatings and Industrial Applications*, Boca Raton, CRC Press, pp. 827–870, 2000.
- [18] STRAEDE, C.A., “Application of ion implantation in tooling industry”, *Nuclear Instruments & Methods in Physics Research. Section B, Beam Interactions with Materials and Atoms*, v. 113, n. 1–4, pp. 161–166, 1996. doi: [http://dx.doi.org/10.1016/0168-583X\(95\)01380-6](http://dx.doi.org/10.1016/0168-583X(95)01380-6).
- [19] LOPES, H.S.M., MORETO, J.A., MANFRINATO, M.D., *et al.*, “Micro abrasive wear behaviour study of carburization and ion plasma nitriding of P20 steel”, *Materials Research*, v. 19, n. 3, pp. 686–694, 2016. doi: <http://dx.doi.org/10.1590/1980-5373-MR-2015-0721>.
- [20] ALMEIDA, L.S., SOUZA, A.R.M., COSTA, L.H., *et al.*, “Effect of nitrogen in the properties of diamond-like carbon (DLC) coating on Ti6 Al4 V substrate”, *Materials Research Express*, v. 7, n. 6, pp. 065601, 2020. doi: <http://dx.doi.org/10.1088/2053-1591/ab94fb>.
- [21] ALTAY, O., GURGENC, T., ULAS, M., *et al.*, “Prediction of wear loss quantities of ferro-alloy coating using different machine learning algorithms”, *Friction*, v. 8, n. 1, pp. 107–114, 2020. doi: <http://dx.doi.org/10.1007/s40544-018-0249-z>.
- [22] BUCHANAN, F.J., SHIPWAY, P.H., “Microabrasion – a simple method to assess surface degradation of UHMWPE following sterilisation and ageing”, *Biomaterials*, v. 23, n. 1, pp. 93–100, 2002. doi: [http://dx.doi.org/10.1016/S0142-9612\(01\)00083-7](http://dx.doi.org/10.1016/S0142-9612(01)00083-7). PubMed PMID: 11762860.
- [23] MARQUES, F.P., SCANDIAN, C., BOZZI, A.C., *et al.*, “Formation of a nanocrystalline recrystallized layer during microabrasive wear of a cobalt-chromium based alloy (Co-30Cr-19Fe)”, *Tribology International*, v. 116, pp. 105–112, 2017. doi: <http://dx.doi.org/10.1016/j.triboint.2017.07.006>.
- [24] COZZA, R.C., “Study of the steady state of wear in micro-abrasive wear testes by rotative ball conducted on specimen of WC–Co P20 and M2 tool-steel”, *Matéria (Rio de Janeiro)*, v. 23, n. 1, pp. e–11986, 2018. doi: <http://dx.doi.org/10.1590/s1517-707620170001.0322>.
- [25] KRELLING, A.P., TEIXEIRA, F., COSTA, C.E., *et al.*, “Microabrasive wear behavior of borided steel abraded by SiO₂ particles”, *Journal of Materials Research and Technology*, v. 8, n. 1, pp. 766–776, 2019. doi: <http://dx.doi.org/10.1016/j.jmrt.2018.06.004>.
- [26] SIQUEIRA, R.C., ALMEIDA, L.S., MANFRINATO, M.D., *et al.*, “The influence of temperature on the tribological properties of the Ti6Al4V alloy treated by plasma oxidation”, *Materials Science Forum*, v. 1012, pp. 418–423, 2020. doi: <http://dx.doi.org/10.4028/www.scientific.net/MSF.1012.418>.
- [27] CAMPOS, L.A.P., ALMEIDA, L.S., SILVA, B.P., *et al.*, “Evaluation of nitriding, nitrocarburizing, organosilicon interlayer, diamond-like carbon film and duplex plasma treatment in the wear and corrosion resistance of AISI 4340 steel”, *Journal of Materials Engineering and Performance*, v. 29, n. 12, pp. 8107–8121, 2020. doi: <http://dx.doi.org/10.1007/s11665-020-05277-9>.
- [28] FERNANDES, F.A.P., HECK, S.C., PICONE, C.A., *et al.*, “On the wear and corrosion of plasma Nitrided AISI, H13”, *Surface and Coatings Technology*, v. 381, pp. 125–216, 2020. doi: <http://dx.doi.org/10.1016/j.surfcoat.2019.125216>.
- [29] STACHOWIAK, G.B., STACHOWIAK, G.W., CELLIERS, O., “Ball-cratering abrasion tests of high-Cr white cast irons”, *Tribology International*, v. 38, n. 11–12, pp. 1076–1087, 2005. doi: <http://dx.doi.org/10.1016/j.triboint.2005.07.035>.

- [30] SANTOS, W.C., PEREIRA NETO, J.O., SILVA, R.O., *et al.*, “Apparatus development and study of abrasive microwear behavior of quenched and tempered AISI 420 steel”, *Matéria (Rio de Janeiro)*, v. 20, n. 2, pp. 304–315, 2015. doi: <http://dx.doi.org/10.1590/S1517-707620150002.0031>.
- [31] RUTHERFORD, K.L., HUTCHINGS, I.M., “A micro-abrasive wear test with particular application to coated systems”, *Surface and Coatings Technology*, v. 79, n. 1–3, pp. 231–239, 1996. doi: [http://dx.doi.org/10.1016/0257-8972\(95\)02461-1](http://dx.doi.org/10.1016/0257-8972(95)02461-1).
- [32] COZZA, R.C., RECCO, A.A.C., TSCHIPTSCHIN, A.P., *et al.*, “Análise comportamental dos coeficientes de atrito e desgaste de sistemas revestidos a desgaste micro-abrasivo”, *Tecnologica em Metalurgia, Materiais e Mineração*, v. 6, n. 4, pp. 237–244, 2010. doi: <http://dx.doi.org/10.4322/tmm.00604010>.
- [33] PEREIRA NETO, J.O., SILVA, R.O., SILVA, E.H., *et al.*, “Wear and corrosion study of plasma nitriding F53 super duplex stainless steel”, *Materials Research*, v. 19, n. 6, pp. 1241–1252, 2016. doi: <http://dx.doi.org/10.1590/1980-5373-mr-2015-0656>.
- [34] TREZONA, R.I., ALLSOPP, D.N., HUTCHINGS, I.M., “Transitions between two- body and three-body abrasive wear: influence of test conditions in the microscale abrasive wear test”, *Wear*, v. 225–229, pp. 205–214, 1999. doi: [http://dx.doi.org/10.1016/S0043-1648\(98\)00358-5](http://dx.doi.org/10.1016/S0043-1648(98)00358-5).
- [35] MCKENZIE, B.M., BRAGA, R.A., COELHO, D.E.C., *et al.*, “Moiré as a low-cost, robust, optical-technique to quantify soil surface condition”, *Soil & Tillage Research*, v. 158, pp. 147–155, 2016. doi: <http://dx.doi.org/10.1016/j.still.2015.12.013>.
- [36] SHOU, Y., LI, K., LIANG, H., *et al.*, “Information hiding scheme based on optical moiré-pixel matrix”, *Optics Communications*, v. 437, pp. 403–407, 2019. doi: <http://dx.doi.org/10.1016/j.optcom.2018.12.043>.
- [37] LAY, Y.L., YANG, H.J., LIN, C.S., *et al.*, “3D face recognition by shadow moiré”, *Optics & Laser Technology*, v. 44, n. 1, pp. 148–152, 2012. doi: <http://dx.doi.org/10.1016/j.optlastec.2011.06.009>.
- [38] ARA, M.H.M., JAVADI, Z., SIROHI, R.S., “Measurement of nonlinear refractive index of Ag and Au nano-particles using moiré technique”, *Optik (Stuttgart)*, v. 122, n. 21, pp. 1961–1964, 2011. doi: <http://dx.doi.org/10.1016/j.ijleo.2010.11.025>.
- [39] COSTA, R.M., BRAGA, R.A., OLIVEIRA, B.S., *et al.*, “Sensitivity of the moiré technique for measuring biological surfaces”, *Biosystems Engineering*, v. 100, n. 3, pp. 321–328, 2008. doi: <http://dx.doi.org/10.1016/j.biosystemseng.2008.04.011>.
- [40] CRUZ, D., SOUZA, B.A., CAMPOS, L.A.P., *et al.*, “Projeto, construção e comissionamento de um reator para tratamento de nitretação iônica a plasma em aço P20”, *Revista Brasileira de Aplicações de Vácuo*, v. 37, n. 3, pp. 102–113, 2018. doi: <https://doi.org/10.17563/rbav.v37i3.1107>.
- [41] ROBERTSON, J., “Diamond-like amorphous carbon”, *Materials Science and Engineering R Reports*, v. 37, n. 4–6, pp. 129–138, 2002. doi: [http://dx.doi.org/10.1016/S0927-796X\(02\)00005-0](http://dx.doi.org/10.1016/S0927-796X(02)00005-0).
- [42] CASIRAGHI, C., FERRARI, A.C., ROBERTSON, J., “Raman spectroscopy of hydrogenated amorphous carbons”, *Physical Review B: Condensed Matter and Materials Physics*, v. 72, n. 8, pp. 085401, 2005. doi: <https://doi.org/10.1103/PhysRevB.72.085401>.
- [43] RANGEL, U.D.O.D., BORGES, R., OLIVEIRA, D.A., *et al.*, “Corrosion and micro-abrasive wear behaviour of 2524-T3 aluminium alloy with PAni-NPs/PSS LbL coating”, *Materials Research*, v. 22, n. 3, pp. 1–9, 2019. doi: <http://dx.doi.org/10.1590/1980-5373-mr-2018-0593>.
- [44] COZZA, R.C., TANAKA, D.K., SOUZA, R.M., “Friction coefficient and abrasive wear modes in ball-cratering tests conducted at constant normal force and constant pressure-preliminary results”, *Wear*, v. 267, n. 1–4, pp. 61–70, 2009. doi: <http://dx.doi.org/10.1016/j.wear.2009.01.055>.
- [45] DAL FABRO, I.M., GAZZOLA, J., DÁVILLA, E., *et al.*, “Physical and mechanical properties of biological materials”, *Revista Ciência Agronômica*, v. 51, n. special, pp. e20207780, 2020. doi: <https://doi.org/10.5935/1806-6690.20200099>.
- [46] CHEN JUNIOR, Y.-C., CHEN, J.-Y., “Optical inspection system for gear tooth surfaces using a projection moiré method”, *Sensors (Basel)*, v. 19, n. 6, pp. 1450, 2019. doi: <http://dx.doi.org/10.3390/s19061450>.
- [47] SANTOS, J.E.B., GAZZOLA, J., SANTANA, T.C., *et al.*, “Classification of oranges by way through the Moiré technique per phase-shifting”, *Brazilian Journal of Development*, v. 6, n. 7, pp. 48049–48059, Jul. 2020. doi: <http://dx.doi.org/10.34117/bjdv6n7-448>.

- [48] LINO, A.C.L., DAL FABBRO, I.M., “Determinação da topografia de uma fruta pela técnica de Moiré de sombra com multiplicação de franjas”, *Ciência e Agrotecnologia*, v. 28, n. 1, pp. 119–125, 2004. doi: <http://dx.doi.org/10.1590/S1413-70542004000100016>.
- [49] COSTA, R.M., “Proposta de um processo de captura e análise de imagens para determinação de forma e superfície de materiais biológicos pela técnica de Moiré”, Monografia de Graduação, Departamento de Ciências da Computação, Universidade Federal de Lavras, Lavras, Minas Gerais, 2006.
- [50] RODRIGUES, S., SANTANA, T.C., GAZZOLA, J., *et al.*, “Application of a shadow Moiré optical technique to generate isodeformation curves on cashew nuts surface”, *International Journal of Science and Engineering Investigations*, v. 4, n. 44, pp. 1–4, 2015.
- [51] YANG, M., “Nitriding – fundamentals, modeling and process optimization”, D.Sc. Thesis, Worcester Polytechnic Institute, Worcester, Massachusetts, United States, 2012.
- [52] DANELON, M.R., SOARES, F., MANFRINATO, M.D., *et al.*, “Study of the effect of the plasma ionic nitriding parameters in wear resistance of SAE 1020 steel used in forming die”, *Revista Brasileira de Aplicações de Vácuo*, v. 39, n. 2, pp. 142–155, 2020. doi: <http://dx.doi.org/10.17563/rbav.v39i2.1166>.
- [53] EDENHOFER, B., “Physical and metallurgical aspects of lonitriding”, *Heat Treatment of Metals*, v. 1, n. 2, pp. 59–67, 1974.
- [54] BASSO, R.L.O., CANDAL, R.J., FIGUEROA, C.A., *et al.*, “Influence of microstructure on the corrosion behavior of nitrocarburized AISI H13 tool steel obtained by pulsed DC plasma”, *Surface and Coatings Technology*, v. 203, n. 10–11, pp. 1293–1297, 2009. doi: <http://dx.doi.org/10.1016/j.surfcoat.2008.10.006>.
- [55] RASTKAR, A.R., KIANI, A., ALVAND, F., *et al.*, “Effect of pulsed plasma nitriding on mechanical and tribological performance of Ck45 steel”, *Journal of Nanoscience and Nanotechnology*, v. 11, n. 6, pp. 5365–5373, 2011. doi: <http://dx.doi.org/10.1166/jnn.2011.3771>. PubMed PMID: 21770190.
- [56] FOLLE, L.F., SCHAEFFER, L., “Evaluation of the tribological conditions in sheet metal forming through bending under tension test”, *Matéria (Rio de Janeiro)*, v. 22, n. 2, pp. 2–15, 2017. <https://doi.org/10.1590/S1517-707620170002.0141>.
- [57] FRATINI, L., LO CASTO, S., LO VALVO, E., “A technical note on an experimental device to measure friction coefficient in sheet metal forming”, *Journal of Materials Processing Technology*, v. 172, n. 1, pp. 16–21, 2006. doi: <http://dx.doi.org/10.1016/j.jmatprotec.2005.08.008>.
- [58] ROSA, A.G.A., MORETO, J.A., MANFRINATO, M.D., *et al.*, “Study on friction and wear behavior of SAE 1045 steel, reinforced nylon 6.6 and NBR rubber used in clutch disks”, *Materials Research*, v. 17, n. 6, pp. 1397–1403, 2014. doi: <http://dx.doi.org/10.1590/1516-1439.282714>.
- [59] NEUBAUER, F., MERKLEIN, M., “Tribological and thermal investigation of modified hot stamping tools”, *Tribology in Industry*, v. 41, n. 1, pp. 76–89, 2019. doi: <http://dx.doi.org/10.24874/ti.2019.41.01.09>.
- [60] KAMARIS, B., “Wear properties of steels plasma nitrided at high temperatures”, *Materials Science and Engineering*, n. 168, n. 1, pp. 49–53, 1993. doi: [https://doi.org/10.1016/0921-5093\(93\)90269-K](https://doi.org/10.1016/0921-5093(93)90269-K).
- [61] KOKHNENKO, N.S., KARPUNIN, I.I., KUZ’MICH, V.V., “Study of reliability for main components and devices of die-cutting presses for packaging”, *Sciences et Techniques (Paris)*, v. 19, n. 4, pp. 320–328, 2020. doi: <http://dx.doi.org/10.21122/2227-1031-2020-19-4-320-328>.
- [62] SEN, U., “Friction and wear properties of thermo-reactive diffusion coatings against titanium nitride coated steels”, *Materials & Design*, v. 26, n. 2, pp. 167–174, 2005. doi: <http://dx.doi.org/10.1016/j.matdes.2004.05.010>.